

# Chemically Induced Expansion of $\text{La}_2\text{NiO}_{4+\delta}$ -Based Materials

Vladislav V. Kharton,<sup>\*,†,‡</sup> Andrei V. Kovalevsky,<sup>†</sup> Maxim Avdeev,<sup>§</sup> Ekaterina V. Tsipis,<sup>†,||</sup> Mikhail V. Patrakeev,<sup>⊥</sup> Aleksey A. Yaremchenko,<sup>†</sup> Eugene N. Naumovich,<sup>†,‡</sup> and Jorge R. Frade<sup>†</sup>

Department of Ceramics and Glass Engineering, CICECO, University of Aveiro, 3810-193 Aveiro, Portugal, Institute of Physicochemical Problems, Belarus State University, 14 Leningradsкая Street, 220050 Minsk, Belarus, The Bragg Institute, Australian Nuclear Science and Technology Organization, PMB 1, Menai, NSW 2234, Australia, Chemistry Department, ITN/CFMC-UL, Estrada Nacional 10, P-2686-953 Sacavém, Portugal; <sup>§</sup> Institute of Solid State Chemistry, Ural Division of the Russian Academy of Science, 91 Pervomayskaya Street, Ekaterinburg 620219, Russia

Received January 11, 2007. Revised Manuscript Received February 16, 2007

The equilibrium chemical strains induced by the oxygen hyperstoichiometry variations in mixed-conducting  $\text{La}_2\text{Ni}_{1-x}\text{M}_x\text{O}_{4+\delta}$  ( $\text{M} = \text{Fe}, \text{Co}, \text{Cu}$ ;  $x = 0\text{--}0.2$ ) with  $\text{K}_2\text{NiF}_4$ -type structure, were studied by controlled-atmosphere dilatometry at 923–1223 K in the oxygen partial pressure range  $5 \times 10^{-4}$  to 0.7 atm. In combination with the oxygen content measured by coulometric titration and thermogravimetry, the results reveal a very low chemical expansivity, favorable for high-temperature electrochemical applications. Under oxidizing conditions, the isothermal expansion relative to atmospheric oxygen pressure ( $\epsilon_c$ ) is less than 0.02%. The ratio between these values and the corresponding nonstoichiometry increment varies from  $-3 \times 10^{-3}$  to  $6 \times 10^{-3}$ , which is much lower compared to most permeable mixed conductors derived from perovskite-like cobaltites and ferrites. Consequently, the chemical contribution to apparent thermal expansion coefficients at a fixed oxygen pressure,  $(13.7\text{--}15.1) \times 10^{-6} \text{ K}^{-1}$ , does not exceed 5%. The high-temperature X-ray diffraction studies showed that this behavior results from strongly anisotropic expansion of the  $\text{K}_2\text{NiF}_4$ -type lattice, namely the opposing variations of the unit-cell parameters on changing oxygen stoichiometry.

## 1. Introduction

Mixed conductors derived from the  $\text{K}_2\text{NiF}_4$ -type lanthanum nickelate,  $\text{La}_2\text{NiO}_{4+\delta}$ , attract a significant attention as promising materials for solid oxide fuel cell (SOFC) cathodes and ceramic membranes for oxygen separation and partial oxidation of light hydrocarbons.<sup>1–9</sup> Important advantages of  $\text{La}_2\text{NiO}_4$ -based compositions include relatively high oxygen-ionic and p-type electronic conductivities, moderate thermal expansion coefficients (TECs), and high electrocatalytic

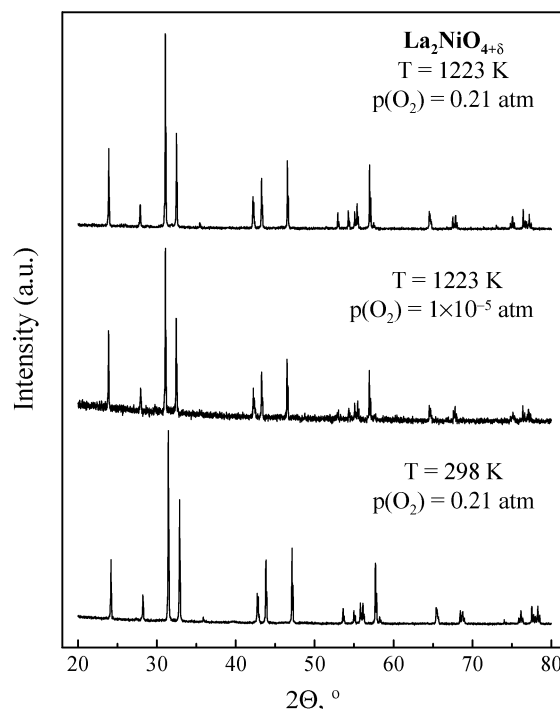


**Figure 1.** Examples of the XRD patterns of  $\text{La}_2\text{NiO}_{4+\delta}$  at various temperatures and oxygen partial pressures.

activity under oxidizing conditions. The oxygen permeation through dense nickelate membranes is essentially limited by kinetics of redox processes at the surface,<sup>1,3,6</sup> which prevents bulk decomposition and enables stable operation under air/

\* Corresponding author. Tel: 351-234-370263. Fax: 351-234-425300. E-mail: kharton@cv.ua.pt.

<sup>†</sup> University of Aveiro.

<sup>‡</sup> Belarus State University.

<sup>§</sup> Australian Nuclear Science and Technology Organization.

<sup>||</sup> ITN/CFMC-UL.

<sup>⊥</sup> Ural Division of the Russian Academy of Science.

- (1) Vigeland, B.; Glenne, R.; Breivik, T.; Julsrud, S. Int. Patent Application PCT WO 99/59702, 1999.
- (2) Skinner, S. J.; Kilner, J. A. *Solid State Ionics* **2000**, *135*, 709.
- (3) Kharton, V. V.; Viskup, A. P.; Naumovich, E. N.; Marques, F. M. B. *J. Mater. Chem.* **1999**, *9*, 2623.
- (4) Kharton, V. V.; Yaremchenko, A. A.; Valente, A. A.; Sobyenin, V. A.; Belyaev, V. D.; Semin, G. L.; Veniaminov, S. A.; Tsipis, E. V.; Shaula, A. L.; Frade, J. R.; Rocha, J. *Solid State Ionics* **2005**, *176*, 781.
- (5) Zhu, D. C.; Xu, X. Y.; Feng, S. J.; Liu, W.; Chen, C. S. *Catal. Today* **2003**, *82*, 151.
- (6) Kharton, V. V.; Tsipis, E. V.; Yaremchenko, A. A.; Frade, J. R. *Solid State Ionics* **2004**, *166*, 327.
- (7) Boehm, E.; Bassat, J. M.; Steil, M. C.; Dordor, P.; Mauvy, F.; Grenier, J. C. *Solid State Sci.* **2003**, *5*, 973.
- (8) Al Daroukh, M.; Vashook, V. V.; Ullmann, H.; Tietz, F.; Arual Raj, I. *Solid State Ionics* **2003**, *158*, 141.
- (9) Aguadero, A.; Alonso, J. A.; Martinez-Lope, M. J.; Fernandez-Diaz, M. T.; Escudero, M. J.; Daza, L. *J. Mater. Chem.* **2006**, *16*, 3402.

**Table 1. Average Linear TECs of La<sub>2</sub>NiO<sub>4</sub>-Based Materials, Calculated from the Dilatometric Data in Different Temperature Ranges, and Estimated Ratio between the True and Apparent TECs**

composition	T range (K)	p(O <sub>2</sub> ) (atm)	$\bar{\alpha} \times 10^6$ (K <sup>-1</sup> )	$\bar{\alpha}_T/\bar{\alpha} \times 100\%$ ( $\pm 1\%$ ) <sup>a</sup>
La <sub>2</sub> NiO <sub>4+δ</sub>	373–723	0.21	13.7	
	923–1223	0.21	14.4	95
	923–1223	$4.8 \times 10^{-3}$	14.7	97
	923–1223	$5.5 \times 10^{-4}$	14.8	97
La <sub>2</sub> Ni <sub>0.9</sub> Fe <sub>0.1</sub> O <sub>4+δ</sub>	373–1123	0.21	13.8	
	1123–1323	0.21	15.1	
	923–1223	0.21	14.6	~100
	923–1223	$6.5 \times 10^{-4}$	14.9	99
La <sub>2</sub> Ni <sub>0.9</sub> Co <sub>0.1</sub> O <sub>4+δ</sub>	373–1123	0.21	13.8	
	923–1223	0.21	14.9	98
	923–1223	$6.5 \times 10^{-4}$	15.1	96
	923–1223	0.21	14.3	~100
La <sub>2</sub> Ni <sub>0.8</sub> Cu <sub>0.2</sub> O <sub>4+δ</sub>	373–1253	0.21	14.2	
	923–1223	0.21	14.3	~100
	923–1223	$6.5 \times 10^{-4}$	14.6	99

<sup>a</sup>  $\bar{\alpha}_T$  is the estimated true TEC, corrected for oxygen nonstoichiometry changes at fixed p(O<sub>2</sub>).

CH<sub>4</sub> gradients up to temperatures as high as 1173 K.<sup>4</sup> At the same time, partial reduction of the membrane surface exposed to a reducing atmosphere results in the formation of a porous La<sub>2</sub>O<sub>3</sub>-supported Ni catalyst layer, providing a high selectivity toward partial oxidation of methane.<sup>5</sup> The thermal expansion of La<sub>2</sub>NiO<sub>4</sub>-based materials is compatible with that for doped ceria and lanthanum gallate,<sup>2–4,6–8</sup> well-known solid electrolytes promising for intermediate-temperature SOFCs.

In addition to appropriate transport and electrocatalytic properties, mixed-conducting materials for SOFC electrodes and ceramic membranes should possess chemical and structural integrity within a wide range of temperature and oxygen partial pressure, p(O<sub>2</sub>). Such requirements are often incompatible, thus limiting the applicability of known systems with fast ionic and electronic transport. As an example, perovskite-like solid solutions based on (Sr,Ln)(Co,Fe)O<sub>3–δ</sub> exhibit attractively high oxygen permeation but are thermodynamically and/or dimensionally unstable under large oxygen chemical potential gradients.<sup>10,11</sup> Losses of lattice oxygen under reducing environments and subsequent changes in the oxidation state of transition metal cations result in unfavorable expansion of the lattice and differential strain across the membrane. A similar situation is typical for oxide cathodes, in which high current densities cause oxygen nonstoichiometry gradients and the corresponding chemical strains.<sup>12</sup> These processes all induce mechanical stresses that may lead to fracture of the membrane ceramics and cracking and delamination of the porous electrodes. Due to changes in oxygen stoichiometry on thermal cycling, chemical expansion may also affect the materials compatibility and dimensional stability in the high-temperature electrochemical devices if even the oxygen chemical potential is fixed, by contributing to the apparent thermal expansion.<sup>13,14</sup> Furthermore, general correlations between the thermal and chemical expansivities, ion diffusivity and oxygen thermodynamic functions are often observed,<sup>8,14–18</sup> as all these properties are governed by the metal–oxygen bonding energy.

Continuing our research on lanthanum nickelate-based mixed conductors,<sup>3,4,6,19</sup> the present work is focused on the study of isothermal chemically induced expansion of La<sub>2</sub>Ni(M)O<sub>4+δ</sub> (M = Fe, Co, and Cu) under oxidizing conditions.

The data on oxygen nonstoichiometry, used for the analysis of chemical strains, were reported in previous publications.<sup>19,20</sup>

## 2. Experimental Section

Single-phase ceramic samples of La<sub>2</sub>Ni<sub>1–x</sub>M<sub>x</sub>O<sub>4+δ</sub> (M = Fe, Co, Cu; x = 0–0.2) with 95–98% density were prepared via a glycine–nitrate synthesis route with sintering at 1500–1730 K in air. A detailed description of the processing conditions and the results of structural characterization of the K<sub>2</sub>NiF<sub>4</sub>-type phases at room temperature can be found elsewhere.<sup>6,19,20</sup> After sintering, all materials were annealed at 1250–1300 K in air and slowly cooled in order to achieve equilibrium oxygen content at low temperatures; the powdered samples for X-ray diffraction (XRD) analysis and oxygen nonstoichiometry measurements were prepared by grinding of dense ceramics. XRD patterns were collected using a Philips X'Pert Pro instrument (CuK<sub>α</sub> radiation, 2θ = 10–80°, step 0.015°, Anton Paar HTK-2000 heating stage) at 300–1223 K in atmospheric air and in a flow of high-purity argon, where the oxygen partial pressure was approximately  $1 \times 10^{-5}$  atm. At each temperature, three 1 h data sets were collected and found identical, thus indicating that an equilibrium state is achieved. The Rietveld refinement was carried out using the GSAS suite with EXPGUI frontend.<sup>21,22</sup> The XRD studies confirmed the stability of all the K<sub>2</sub>NiF<sub>4</sub>-type phases in the whole range of conditions in which dilatometric measurements were performed, as expected. Examples of the XRD patterns for undoped La<sub>2</sub>NiO<sub>4+δ</sub> are presented in Figure

- (10) Pei, S.; Kleefisch, M. S.; Kobylinski, T. P.; Faber, J.; Udovich, C. A.; Zhang-McCoy, V.; Dabrowski, B.; Balachandran, U.; Mievile, R. L.; Poeppel, R. B. *Catal. Lett.* **1995**, *30*, 201.
- (11) Schwartz, M.; White, J. H.; Sammells, A. F. U.S. Patent 6214757, 2001.
- (12) Bieberle, A.; Gauckler, L. J. In *Oxygen Ion and Mixed Conductors and Their Technological Applications*; Tuller, H. L., Schoonman, J., Riess, I., Eds.; Kluwer Academic Publishers: Dordrecht, The Netherlands, 2000; 347.
- (13) Adler, S. B. *J. Am. Ceram. Soc.* **2001**, *84*, 2117.
- (14) Kharton, V. V.; Yaremchenko, A. A.; Patrakee, M. V.; Naumovich, E. N.; Marques, F. M. B. *J. Eur. Ceram. Soc.* **2003**, *23*, 1417.
- (15) Ullmann, H.; Trofimenko, N.; Tietz, F.; Stover, D.; Ahmad-Khanlou, A. *Solid State Ionics* **2000**, *138*, 79.
- (16) Hayashi, H.; Suzuki, M.; Inaba, H. *Solid State Ionics* **2000**, *128*, 131.
- (17) Chen, X.; Yu, J.; Adler, S. B. *Chem. Mater.* **2005**, *17*, 4537.
- (18) Kharton, V. V.; Naumovich, E. N.; Yaremchenko, A. A.; Marques, F. M. B. *J. Solid State Electrochem.* **2001**, *5*, 160.
- (19) Naumovich, E. N.; Patrakee, M. V.; Kharton, V. V.; Yaremchenko, A. A.; Logvinovich, D. I.; Marques, F. M. B. *Solid State Sci.* **2005**, *7*, 1353.
- (20) Tsipis, E. V.; Naumovich, E. N.; Patrakee, M. V.; Waerenborgh, J. C.; Pivak, Y. V.; Gaczyński, P.; Kharton, V. V. *J. Phys. Chem. Solids* **2007**, submitted.

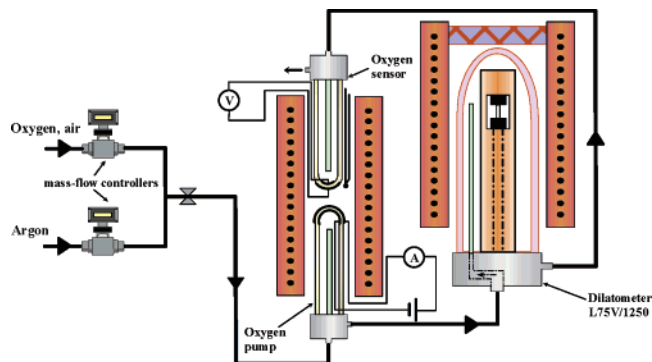


**Figure 2.** Experimental setup for measurement of thermal and chemically induced expansion.

1. The overall cation composition of selected ceramic samples was verified by ion-coupled plasma (ICP) spectroscopic analysis. The energy dispersive spectroscopy (EDS) combined with scanning and transmission electron microscopy (SEM and TEM) showed an absence of compositional inhomogeneities, within the limits of experimental uncertainty. The experimental techniques and equipment used for characterization were described in previous publications.<sup>3,4,6,14,19</sup> The total oxygen content was determined in the oxygen pressure range  $1 \times 10^{-5}$  to 0.7 atm at 923–1223 K by the coulometric titration (CT) and thermogravimetric analysis (TGA).<sup>19</sup> The data on steady-state oxygen permeation through dense nickelate membranes, used in this work for comparison, were collected as reported elsewhere.<sup>3</sup>

The experimental setup for the measurements of thermal and chemically induced expansion of  $\text{La}_2\text{NiO}_4$ -based ceramics (Figure 2) comprised a vertical alumina dilatometer Linseis L75V/1250 and a gas system with an yttria-stabilized zirconia (YSZ) oxygen pump and one YSZ sensor at the outlet. The total gas flow rate ( $\sim 50$  mL/min) and the oxygen partial pressure in the influent  $\text{O}_2$ -Ar and  $\text{O}_2$ - $\text{N}_2$  mixtures, continuously supplied in the dilatometer, were fixed by the electrochemical pump and two Bronkhorst mass-flow controllers; the sensor was used for permanent control of the oxygen chemical potential in the gas flow. The dilatometric studies were performed at 923–1223 K in the oxygen partial pressure range from  $5 \times 10^{-4}$  to 0.7 atm. Before measurements, the dilatometer was calibrated for the necessary temperature profile at each gas composition using alumina as a blank material. The standard procedure included heating to 1243 K, dwelling at a given  $p(\text{O}_2)$  for 5–25 h, and subsequent temperature cycling in the range 923–1223 K with step of 50 K and equilibration at each temperature for 2–7 h. One example illustrating this measurement regime is presented in Figure 3, where the data are given relative to the room-temperature length ( $L_0'$ ); the latter is taken as the reference state suitable for characterization of thermal expansion and for comparison of chemically induced strains at different temperatures.<sup>12,14</sup> Notice that, although the relaxation times after stepwise temperature changes were relatively short (inset in Figure 3), a significant difference in  $\Delta L/L_0'$  values was observed when using the regime with a constant heating/cooling rate, such as 3 K/min (Figure 4). This difference, caused by incomplete equilibration with gas phase under the continuous heating/cooling conditions, makes it impossible to use the latter regime for precise studies of  $\text{La}_2\text{NiO}_4$ -based materials. On the contrary, dimensional changes determined by equilibrating the sample at each temperature show an excellent reproducibility (inset in Figure 4).

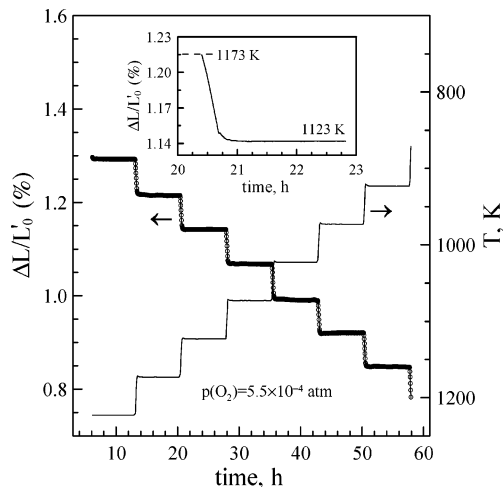


**Figure 3.** Fragment of the dilatometric curve of  $\text{La}_2\text{NiO}_{4+\delta}$  ceramics at  $p(\text{O}_2) = 5.5 \times 10^{-4}$  atm, obtained on temperature cycling at 923–1223 K with equilibration at each temperature. The inset illustrates length relaxation after a change in temperature.

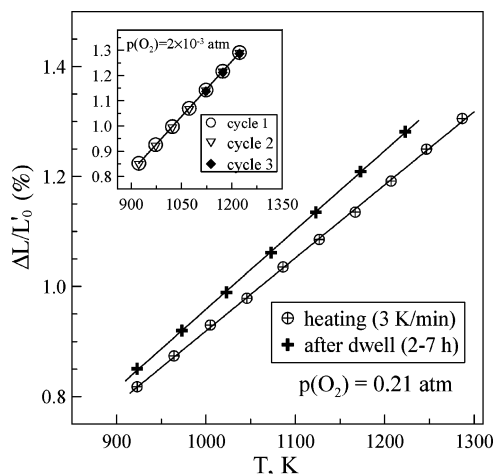


**Figure 4.** Thermal expansion of  $\text{La}_2\text{NiO}_{4+\delta}$  ceramics in air, obtained in the regimes of continuous heating and temperature cycling with 2–7 h dwells at each temperature. The inset illustrates reproducibility of the relative elongation during temperature cycling at  $p(\text{O}_2) = 2 \times 10^{-3}$  atm with equilibration at each temperature. All data are given relative to the room-temperature length ( $L_0'$ ).

### 3. Results and Discussion

Typical temperature dependencies of the oxygen nonstoichiometry and expansion of  $\text{La}_2\text{Ni}(\text{M})\text{O}_{4+\delta}$  ( $\text{M} = \text{Fe}, \text{Co}, \text{Cu}$ ) at a fixed oxygen pressure are presented in Figures 5 and 6. These dependencies are almost linear, in agreement with literature data.<sup>7,23</sup> At 923–1223 K, the average values of linear thermal expansion coefficients ( $\bar{\alpha}$ ) of  $\text{La}_2\text{NiO}_{4+\delta}$  vary in the range  $(14.4\text{--}14.8) \times 10^{-6} \text{ K}^{-1}$ , tending to increase moderately when the oxygen partial pressure decreases (Table 1). Doping with cobalt and iron also leads to a slight increase in the TEC values, whereas the substitution of nickel with copper has an opposite influence. Such changes, and also the substantial variations in oxygen content with temperature, might suggest the presence of a non-negligible chemical contribution to the lattice expansion. In these conditions, the average TECs should be understood as

(21) Toby, B. H. *J. Appl. Crystallogr.* **2001**, *34*, 210.

(22) Larson, A. C.; Von Dreele, R. B. *General Structure Analysis System (GSAS)*; Los Alamos National Laboratory Report LAUR 86-748; Los Alamos National Laboratory: Los Alamos, NM, 2004.

(23) Amow, G.; Davidson, I. J.; Skinner, S. J. *Solid State Ionics* **2006**, *177*, 1205.

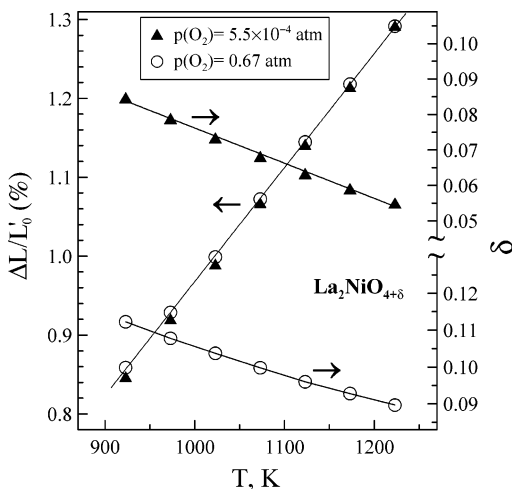


**Figure 5.** Temperature dependence of the relative elongation and oxygen nonstoichiometry of  $\text{La}_2\text{NiO}_{4+\delta}$  at various oxygen partial pressures. The dilatometric data are given relative to the room-temperature length ( $L_0'$ ).

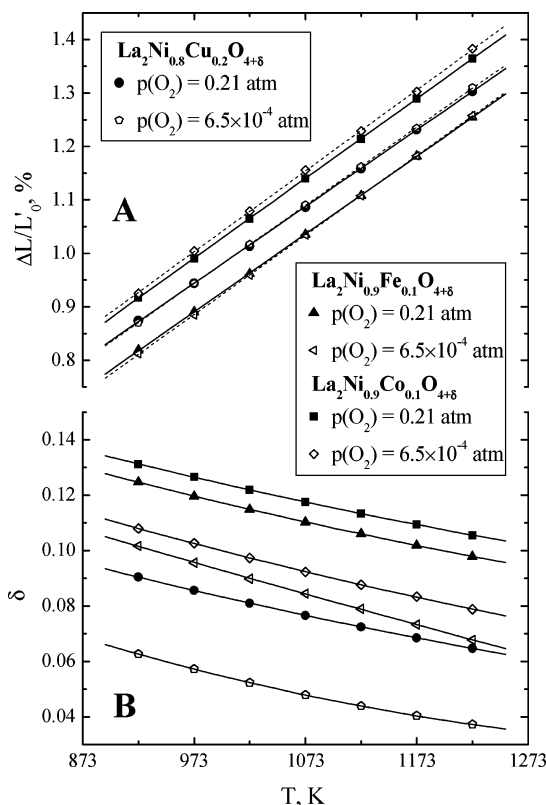


**Figure 6.** Temperature dependence of the relative elongation (A) and oxygen hyperstoichiometry (B) of  $\text{La}_2\text{NiO}_4$ -based materials at various oxygen partial pressures. The dilatometric data are given relative to the room-temperature length ( $L_0'$ ).

apparent, resulting from a combined effect of the true thermal expansion and chemical strain of the lattice. On the other hand, all  $\text{La}_2\text{NiO}_4$ -based materials exhibit modest dimensional changes on varying  $p(\text{O}_2)$  at a given temperature, which are much lower than those of  $(\text{La},\text{Sr})\text{CoO}_{3-\delta}$  and  $(\text{La},\text{Sr})\text{FeO}_{3-\delta}$  perovskites.<sup>14,17,24</sup> As an illustration, Figure 7 displays the relationships between relative elongation and oxygen hyperstoichiometry of undoped  $\text{La}_2\text{NiO}_{4+\delta}$  as func-

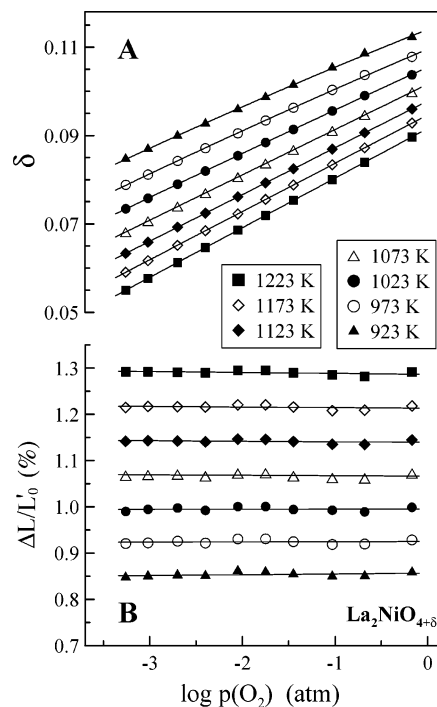


**Figure 7.** Oxygen nonstoichiometry (A) and relative length change (B) of  $\text{La}_2\text{NiO}_{4+\delta}$  ceramics as a function of the oxygen partial pressure. The dilatometric data are given relative to the room-temperature length ( $L_0'$ ).

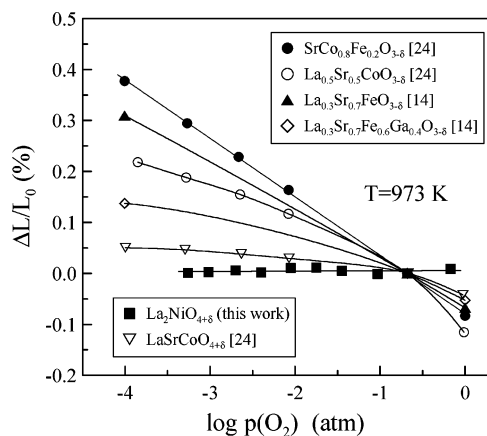


**Figure 8.** Chemically induced strain of  $\text{La}_2\text{NiO}_{4+\delta}$  ceramics, compared to data on cobaltite- and ferrite-based mixed conductors.<sup>14,24</sup> Solid lines are for visual guidance only. The data are given relative to the length at atmospheric oxygen pressure and 973 K.

tion of the oxygen partial pressure. In the  $p(\text{O}_2)$  range from  $5 \times 10^{-4}$  to 0.7 atm, when the isothermal variations in  $\delta$  values at each temperature are in the range 0.027–0.036, the maximum uniaxial expansion does not exceed 0.012%. This level of chemical strain is still higher compared to various  $\text{LaCrO}_3$ -based solid solutions with predominant electronic transport and  $\text{Ce}(\text{Gd})\text{O}_{2-\delta}$  electrolytes under oxidizing conditions,<sup>25,26</sup> but is rather exceptional for mixed conductors and favorable for practical electrochemical applications.

Figure 8 compares the chemical strains of  $\text{La}_2\text{NiO}_{4+\delta}$  and other mixed-conducting ceramics.<sup>14,24</sup> As all data correspond

(24) Vashook, V. V. DSc. Thesis, Institute of General and Inorganic Chemistry, National Belarus Academy of Sciences, Minsk, Belarus, 2000 (in Russian).

(25) Armstrong, T. R.; Stevenson, J. W.; Pederson, L. R.; Raney, P. E. *J. Electrochem. Soc.* **1996**, *143*, 2919.

(26) Wang, S.; Katsuki, M.; Hashimoto, T.; Dokiya, M. *J. Electrochem. Soc.* **2003**, *150*, A952.



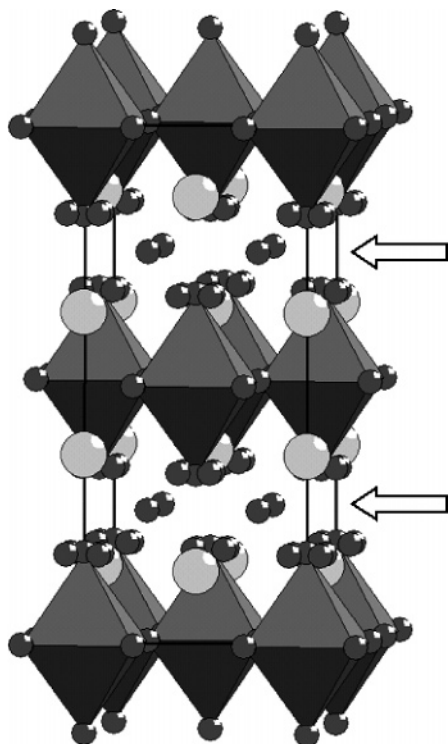


**Figure 9.** Crystal structure of  $\text{La}_2\text{NiO}_{4+\delta}$ , on the basis of neutron diffraction data.<sup>27</sup> The arrows show layers of the interstitial oxygen. Increasing content of extra oxygen ( $\delta$ ) results in expansion of the  $c$ -axis due to anion–anion repulsion and contraction of the  $a$ – $b$  plane due to the decreasing average size of  $\text{Ni}^{2+2\delta}$  cations.

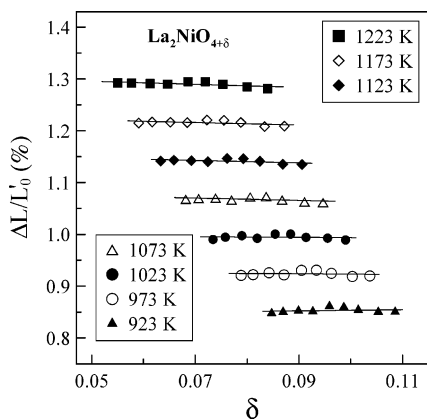


**Figure 10.** Chemical expansion of  $\text{La}_2\text{NiO}_{4+\delta}$  as a function of the oxygen nonstoichiometry, calculated from the data shown in Figure 7.

to 973 K, the reference length ( $L_0$ ) was selected at atmospheric oxygen pressure and the same temperature. Under identical conditions, the isothermal chemically induced expansion of lanthanum nickelate is up to 30–40 times lower than that of perovskite-type  $\text{SrCo}_{0.8}\text{Fe}_{0.2}\text{O}_{3-\delta}$ <sup>24</sup> and  $\text{La}_{0.3}\text{Sr}_{0.7}\text{FeO}_{3-\delta}$ .<sup>14</sup> Such difference in behavior can be easily understood considering the different mechanisms of oxygen deintercalation from these phases. For the  $\text{ABO}_{3-\delta}$  perovskite structure, decreasing  $p(\text{O}_2)$  leads to the formation of oxygen vacancies, charge-compensated by partial reduction of the B-site cations. Both (i) the corresponding increase in the B-site cation radius and (ii) rising coulombic repulsion between the cations expand perovskite lattice. In the case of oxygen-hyperstoichiometric  $\text{A}_2\text{BO}_{4+\delta}$  compounds with layered  $\text{K}_2\text{NiF}_4$ -type structure, such as  $\text{La}_2\text{NiO}_{4+\delta}$ , these two

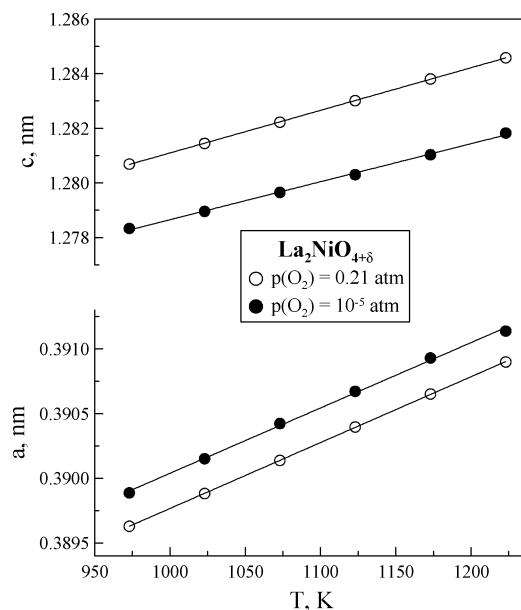


**Figure 11.** Temperature dependence of the tetragonal unit-cell parameters of  $\text{La}_2\text{NiO}_{4+\delta}$ .

factors produce opposite effects on the lattice in the  $ab$ -plane and along the  $c$ -axis. Although dimensional changes in the  $ab$ -plane are still controlled by the size of B-site cations, the chemically induced expansion/contraction of the  $c$  parameter is governed by the amount of hyperstoichiometric oxygen incorporated into rock-salt  $\text{La}_2\text{O}_2$  layers, via anion–anion repulsion (Figure 9). Consequently, oxygen losses from the  $\text{La}_2\text{NiO}_{4+\delta}$  structure results in expansion along the perovskite-like layers due to decreasing Ni oxidation state, and in contraction along the perpendicular  $c$ -axis due to decreasing concentration of  $\text{O}^{2-}$  interstitials. These effects compensate each other and, thus, partly suppress the overall strain, which becomes almost independent of the oxygen stoichiometry (Figure 10). Such a conclusion is consistent with numerous literature data on the chemical expansion of various perovskite- and  $\text{K}_2\text{NiF}_4$ -type materials.<sup>1,8,11–15,17,24,28</sup> Notice also that the minor variations in  $\Delta L/L_0'$  with isothermal changes of the oxygen nonstoichiometry (Figure 10) might be explained in terms of the point-defects repulsion model,<sup>19</sup> which suggests a minimum defect interaction energy at intermediate  $\delta$  values in  $\text{La}_2\text{NiO}_{4+\delta}$ ; the corresponding strains are, however, close to the level of experimental uncertainty and cannot be analyzed quantitatively.

The above hypothesis is validated by the high-temperature XRD data, Figure 11. It should be separately emphasized that  $\text{La}_2\text{NiO}_{4+\delta}$  lattice symmetry can vary from tetragonal (space groups  $I4/mmm$  or  $F4/mmm$ ) to orthorhombic (S.G.  $Fmmm$  and  $Cmca$ ), depending on the oxygen chemical potential and temperature.<sup>27–30</sup> In agreement with literature data, the high-temperature XRD analysis showed that in the whole  $p(\text{O}_2)$  range studied in this work, the structure of  $\text{La}_2$ -

(27) Paulus, W.; Cousson, A.; Dhaleenne, G.; Berthon, J.; Revcolevschi, A.; Hosoya, S.; Treutmann, W.; Heger, G.; Le Toquin, R. *Solid State Sci.* **2002**, *4*, 565.

(28) Rice, D. E.; Buttrey, D. J. *J. Solid State Chem.* **1993**, *105*, 197.

(29) Jorgensen, J.; Dabrowski, B.; Pei, S.; Richards, D.; Hinks, D. *Phys. Rev. B* **1989**, *40*, 2187.

(30) Zhang, Z.; Greenblatt, M. *J. Solid State Chem.* **1995**, *117*, 236.

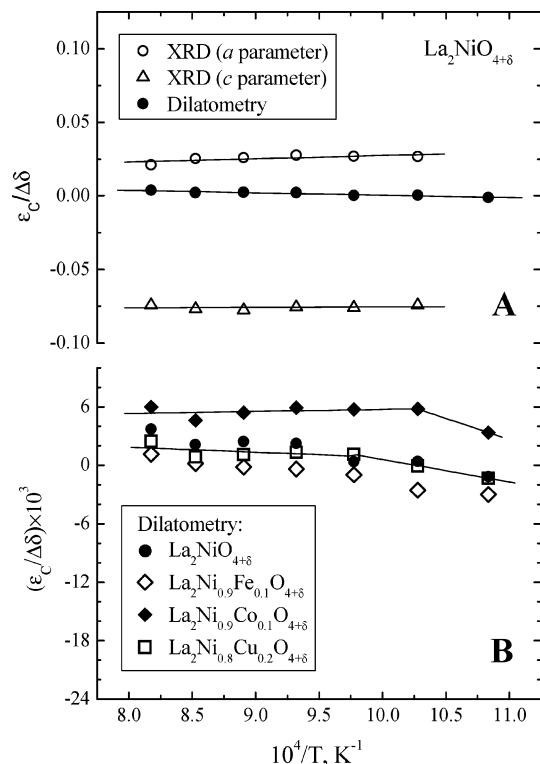


**Figure 12.** Temperature dependence of the  $(\epsilon_c/\Delta\delta)$  coefficients of  $\text{La}_2\text{NiO}_{4+\delta}$  as calculated from dilatometric and high-temperature XRD data at  $p(\text{O}_2) = 1 \times 10^{-5}$  to 0.21 atm (A), and comparison of the  $(\epsilon_c/\Delta\delta)$  values for  $\text{La}_2\text{NiO}_4$ -based materials (B).

$\text{NiO}_{4+\delta}$  is tetragonal, S.G.  $I4/mmm$ . Analogous conclusions were also drawn for all  $\text{La}_2\text{NiO}_4$ -based solid solutions at temperatures above 900 K. The data on chemical expansion, summarized in this manuscript, correspond therefore to tetragonal  $\text{K}_2\text{NiF}_4$ -type phases with a significant oxygen hyperstoichiometry. As for the dilatometric data, both parameters of the tetragonal unit cell of  $\text{La}_2\text{NiO}_{4+\delta}$  exhibit essentially linear dependencies on temperature (Figure 11). In spite of the structure anisotropy, the average linear TECs estimated roughly from the volume expansion coefficients ( $\beta$ ) using the well-known ratio for isotropic lattices,  $\bar{\alpha} = \beta/3$ , are highly compatible with the dilatometric data. For instance, the  $(\beta/3)$  value at 973–1223 K in air is  $(13.2 \pm 0.1) \times 10^{-6} \text{ K}^{-1}$ . Reducing  $p(\text{O}_2)$  down to  $1 \times 10^{-5}$  atm leads to opposing variations of the unit-cell parameters. Namely, the lattice suffers a significant contraction along the  $c$ -axis, whereas the  $a$  parameter increases. This anisotropic behavior is responsible for the low chemical strains determined by dilatometry (Figure 12A). It is noteworthy that although analogous changes in the  $a$  and  $c$  parameters occur on reduction of other  $\text{K}_2\text{NiF}_4$ -type phases such as  $\text{LaSrNiO}_{4+\delta}$  and  $\text{LaSrCoO}_{4+\delta}$ ,<sup>24</sup> their compensation in  $\text{La}_2\text{NiO}_{4+\delta}$  is almost perfect. Similar phenomena are also known for the thermal expansivity; as a representative example, strongly anisotropic expansion along the  $a$ ,  $b$ , and  $c$  axes of orthorhombic  $\text{Al}_2(\text{WO}_4)_3$  results in very low volume changes on heating.<sup>31</sup>

The chemical contribution to the apparent thermal expansion coefficients at fixed  $p(\text{O}_2)$  can be estimated assuming that the strain ( $\epsilon_c = \Delta L/L_0$ ) is a linear function of the oxygen nonstoichiometry variations under isothermal conditions. The latter approach can be considered as a first approximation only,<sup>32</sup> but enables us to quantitatively compare chemically induced expansion in materials with different nonstoichiometry and defect chemistry.<sup>33</sup> Using this linearized model and the dilatometric and coulometric-titration data (Figures 5 and 6), one may calculate the true TEC values ( $\bar{\alpha}_T$ ) in a given temperature range by the relationship<sup>14</sup>

$$\bar{\alpha}_T = \frac{\bar{\alpha}\Delta T - \gamma\Delta\delta}{(\gamma\Delta\delta + 1)\Delta T} \quad (1)$$

where  $\gamma = (\epsilon_c/\Delta\delta)_T$ , the values of  $\bar{\alpha}$  and  $\Delta\delta$  correspond to the temperature increment  $\Delta T$  at a fixed oxygen pressure, and  $\bar{\alpha}_T$  relates to the thermally induced expansion of a sample where the oxygen content is fixed equal to that in the final state. Table 1 lists the ratios between the apparent and true thermal expansion coefficients estimated in such a manner. As expected, chemical contribution to the TEC values measured at constant oxygen pressure is low for all  $\text{La}_2\text{NiO}_4$ -based materials, varying in the range 0–5%. For comparison, in the case of  $\text{La}_{0.3}\text{Sr}_{0.7}\text{Fe}(\text{Ga})\text{O}_{3-\delta}$  perovskites, the corresponding values are as high as 35–50% and tend to increase at a moderate  $p(\text{O}_2)$ .<sup>14</sup>

Comparison of the  $(\epsilon_c/\Delta\delta)_T$  coefficients for undoped  $\text{La}_2\text{NiO}_{4+\delta}$  and its derivatives is presented in Figure 12B. In all cases, these parameters are essentially temperature-independent; although a slight tendency to increase on heating may be mentioned, the corresponding changes are close to the experimental error. The difference in chemical expansivity is also insignificant for all  $\text{La}_2\text{NiO}_4$ -based compositions, except for  $\text{La}_2\text{Ni}_{0.9}\text{Co}_{0.1}\text{O}_{4+\delta}$ , which shows maximum  $(\epsilon_c/\Delta\delta)$  values. Most likely, such a behavior is associated with substantial changes of the cobalt oxidation states in the studied  $p(\text{O}_2)$  range, where the fractions of  $\text{Co}^{2+}$  and  $\text{Co}^{3+}$  in  $\text{La}_2\text{Ni}_{0.9}\text{Co}_{0.1}\text{O}_{4+\delta}$  are comparable.<sup>19</sup> For  $\text{La}_2\text{Ni}_{0.9}\text{Fe}_{0.1}\text{O}_{4+\delta}$ , the dominant state of iron cations in the same conditions is trivalent;<sup>20</sup> the states of copper and nickel cations in  $\text{La}_2\text{Ni}_{0.8}\text{Cu}_{0.2}\text{O}_{4+\delta}$  are statistically indistinguishable.<sup>19</sup> Note that the thermal expansion of perovskite-related cobaltites is also greater than that of their Fe- and Ni-containing analogues, particularly due to changes in the cobalt cation electronic state.<sup>8,34,35</sup>

Finally, literature data<sup>14,15,18,24,34</sup> suggest a general correlation between thermal and chemical expansion and ionic conduction in solids. However, notwithstanding the fact that the expansion of  $\text{K}_2\text{NiF}_4$ -type phases is much lower than that for perovskite-type materials, lanthanum nickelate possesses relatively fast ionic transport. As an example, under similar

(31) Imanaka, N.; Hiraiwa, M.; Adachi, G.; Dabkowska, H.; Dabkowski, A. *J. Cryst. Growth* **2000**, 220, 176.

(32) Atkinson, A. *Solid State Ionics* **1997**, 95, 249.

(33) Atkinson, A.; Ramos, T. M. G. M. *Solid State Ionics* **2000**, 129, 259.

(34) Kharton, V. V.; Yaremchenko, A. A.; Naumovich, E. N. *J. Solid State Electrochem.* **1999**, 3, 303.

(35) Goodenough, J. B.; Zhou, J. S. In *Localized to Itinerant Electronic Transition in Perovskite Oxides*; Goodenough, J.B., Ed.; Springer-Verlag: Berlin, 2001; p 17.

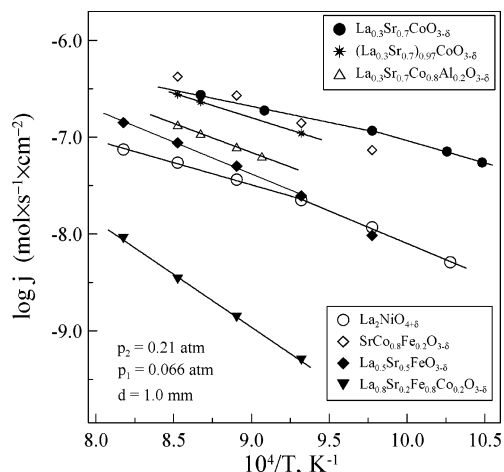


**Figure 13.** Temperature dependence of the oxygen permeation fluxes through planar ceramic membranes made of selected mixed-conducting materials, under a fixed oxygen partial-pressure gradient. All data correspond to membranes without surface modification. The membrane thickness ( $d$ ) and feed-side oxygen pressure ( $p_2$ ) are 1.0 mm and 0.21 atm, respectively. Data from refs 6, 36, and 37 are used for comparison.

conditions, the oxygen permeation fluxes through dense  $\text{La}_2\text{NiO}_{4+\delta}$  ceramics are only 6–10 times lower than those for perovskite-type  $\text{SrCo}_{0.8}\text{Fe}_{0.2}\text{O}_{3-\delta}$  and  $\text{La}_{0.3}\text{Sr}_{0.7}\text{CoO}_{3-\delta}$  (Figure 13), which are among the most permeable materials of mixed-conducting membranes.<sup>34,36</sup> This level of oxygen permeability is comparable to  $\text{La}_{0.5}\text{Sr}_{0.5}\text{FeO}_{3-\delta}$ , a candidate composition of the ceramic membrane reactors for natural gas conversion.<sup>37</sup> At the same time, chemically induced expansion of these perovskites is up to 30–200 times greater than that of  $\text{La}_2\text{NiO}_{4+\delta}$ , depending on the oxygen pressure range and temperature.<sup>14,17,24</sup> Such features of lanthanum nickelate-based materials are advantageous for

the applications in ceramic membranes and SOFCs; further improvements may be achieved by the development of appropriate doping strategies in order to increase concentration of mobile oxygen interstitials without rising oxygen nonstoichiometry variations under the operation conditions.

#### 4. Conclusions

Dense ceramics of  $\text{K}_2\text{NiF}_4$ -type  $\text{La}_2\text{Ni}_{1-x}\text{M}_x\text{O}_{4+\delta}$  ( $\text{M} = \text{Fe}, \text{Co}, \text{Cu}; x = 0-0.2$ ) were prepared via the glycine–nitrate route and studied by controlled-atmosphere dilatometry at 923–1223 K in the oxygen partial pressure range  $5 \times 10^{-4}$  to 0.7 atm. In combination with the oxygen content measured by coulometric titration and thermogravimetry, the results showed a very low chemical expansivity, favorable for high-temperature electrochemical applications. The high-temperature X-ray diffraction studies showed that this behavior results from a strongly anisotropic expansion of the  $\text{K}_2\text{NiF}_4$ -type lattice, namely the opposing changes in the unit cell parameters with oxygen nonstoichiometry. Under oxidizing conditions, the ratio between isothermal linear strain and nonstoichiometry increment in  $\text{La}_2\text{Ni}_{1-x}\text{M}_x\text{O}_{4+\delta}$ ,  $(\epsilon_c/\Delta\delta)$  varies from  $-3 \times 10^{-3}$  to  $6 \times 10^{-3}$ , whereas the chemical expansion relative to the atmospheric oxygen pressure is less than 0.02%. As a result, the chemical contribution to the apparent thermal expansion coefficients at a fixed oxygen pressure does not exceed 5%. The chemical expansivity of  $\text{La}_2\text{NiO}_4$ -based materials is much lower compared to perovskite-like mixed conductors with maximum oxygen permeability and ionic conductivity.

**Acknowledgment.** This work was supported by the FCT, Portugal (Projects POCL/CTM/59197/2004, REEQ/710/CTM/2005, SFRH/BPD/15003/2004, and SFRH/BPD/28629/2006), and the MatSILC project (STRP 033410, CEC). The authors are sincerely grateful to A. Shaula and Y. Pivak for their experimental assistance and helpful discussions.

CM070096X

- (36) Kharton, V. V.; Tsipis, E. V.; Yaremchenko, A. A.; Marozau, I. P.; Viskup, A. P.; Frade, J. R.; Naumovich, E. N. *Mater. Sci. Eng., B* **2006**, *134*, 80.
- (37) Tsipis, E. V.; Patrakeev, M. V.; Kharton, V. V.; Yaremchenko, A. A.; Mather, G. C.; Shaula, A. L.; Leonidov, I. A.; Kozhevnikov, V. L.; Frade, J. R. *Solid State Sci.* **2005**, *7*, 355.